35th Annual International Conference of the IEEE EMBS
Osaka, Japan, 3 - 7 July, 2013

Mapping Activation in a Sinoatrial Node Cardiac Tissue Preparation with a Multi-Electrode Array

Fred Tanyous, Amr Al Abed (*Member, IEEE*), Adrian Bradd, Nigel Lovell (*Fellow, IEEE*) and Socrates Dokos (*Member, IEEE*)

***Abstract*- An isolated rabbit cardiac sinoatrial node (SAN) tissue preparation was used experimentally to map activation times and conduction velocities of extracellular cardiac action potential (AP) propagation. Extracellular recordings were carried out using a two-dimensional array of unipolar Ag-AgCl microelectrodes connected to a 128-channel data acquisition system. A 20th order, low-pass Butterworth filter, with a cut-off frequency of 50 Hz, was used in conjunction with a Matlab algorithm to map activation times and conduction velocities. Results show an initial slow-down of the activation wavefront emanating from the SAN, followed by acceleration in some regions, particularly near the Superior Vena Cava, as it travels towards the SAN periphery.**

I. Introduction

Several theories have been postulated regarding the activation time course of the cardiac action potential (AP) and the preferred conduction paths between the sinoatrial node (SAN) and the atrioventricular node (AVN) [1]. Previous research has suggested two major models of SAN structure. The first, known as the ***gradient model***, suggests that in the SAN region, the intrinsic cellular properties *gradually* change from SAN to atrial myocytes towards the SAN periphery. The second proposal, known as the ***mosaic model***, suggests the existence of a random interspersion of SAN and atrial myocytes, with more SAN cells concentrated at the centre and more atrial cells in the periphery [2]. A 2D multi-electrode array was designed and built to throw light on the activation profile in a rabbit SAN tissue preparation, specifically between the centre of the SAN and its periphery, to clarify the nature of any preferential propagation paths present, as well as assisting in clarifying the nature of SAN structure.

In deducing the activation and conduction velocity maps in and around the periphery of the SAN, we can readily identify any changes in propagation velocity and activation wavefront direction from the SAN centre to the periphery, elucidating any preferred paths for the AP and possibly informing on the type of cells within the SAN region.

Fred Tanyous, Amr Al Abed, Adrian Bradd, Nigel Lovell and Socrates Dokos are with the Graduate School of Biomedical Engineering, the University of New South Wales, Sydney, 2052, Australia. (e-mail: s.dokos@unsw.edu.au)

II. Methods

A printed circuit board containing a matrix of 12x11 unipolar Ag-AgCl hemispherical microelectrodes was designed and built (Figs. 1A & 1B). All electrodes were connected to a 128-channel data acquisition system (Tucker Davis Technologies (TDT) Inc., Alachua, FL, USA). Each microelectrode was 0.1 mm in diameter and spaced 0.7 mm (centre-centre) from adjacent electrodes in a regular square grid. A common ground microelectrode was used, located about 0.5 cm from the electrode array.

For the SAN tissue preparation, a white New Zealand rabbit was anaesethised by a mixture of 5% isoflurane and oxygen. The heart was then rapidly excised and the SAN tissue removed and placed on the microelectrodes, secured by a nylon thread harp. The tissue preparation was superfused with Tyrode's solution of the following composition (in mM): 130 NaCl, 4 KCl, 1.2 $CaCl_2$, 0.5 $MgCl_2$, 1.8 NaH_2PO_4, 18 $NaHCo_3$ & 10 glucose. The solution was bubbled with 95% O_2 and 5% CO_2 to maintain a physiological pH level necessary for normal heart function. The solution temperature was maintained at 35°C, with a flow-rate of 3 mL/min. Sampling rate used in the recordings was 12.2 kHz, enough to capture the rapid changes in extracellular APs, as suggested in previous studies [3]. 128 channels were recorded simultaneously by the TDT data acquisition system.

Fig. 1A: Electrode array board, with bath and connections to the data acquisition system.

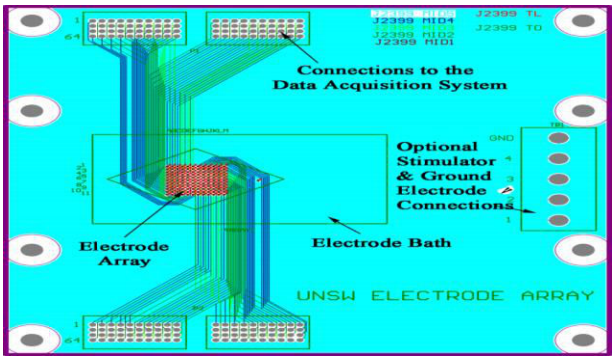

Fig. 1B: Wiring schematic of the electrode board

Raw data consisting of the first six consecutive APs was then imported to Matlab (Mathworks Inc., Natick, MA, USA) as Comma-Separated Value (.csv) files. A custom-written Matlab algorithm was then used to calculate and graph the activation contour map (Fig. 2), the conduction velocity map (Fig. 3) and the velocity vector map (Fig. 4) of the average of the first six beats recorded from the SAN tissue. In order for the contour maps to be drawn, the AP peaks were detected during postprocessing, as described next. The data was filtered first using a low-pass, 20th order, Butterworth filter with a cut-off frequency 50 Hz and then a Matlab function '`findpeaks`' was used. Its format was as follows:

```
[peaks, locs] = findpeaks (mydata1{k}, 'minpeakheight', 0.71 * mean(mydata1{k}), 'minpeakdistance', 7500, 'npeaks', num_of_peaks);
```

Where:

`[peaks, locs]` indicates the value of the peak `(peaks)` and its location `(locs)`.

`mydata1{k}` is the raw data imported from the data acquisition system, with `{k}` indicating the channel number.

`minpeakheight` specifies the minimum acceptable peak height. It was chosen to be a function of the mean raw data imported `(0.71 * mean(mydata1{k}))`.

`minpeakdistance` is the minimum time allowed between 2 peaks, measured in ticks, where 1 tick = 1/(data sampling rate). The value chosen here was `7500 ticks`, suitable with the basal heart rate of the tissue sample.

`npeaks` is the number of peaks to be detected. `num_of_peaks` is an operator-initiated parameter input indicating the number of peaks to be analysed.

The activation contour map (Fig. 2) was plotted by using a sorting algorithm to find the sequence of occurrence of the wave peaks, and then a plot relating the peak times to the peak positions was obtained. The plot shown in Fig. 2 illustrates the activation times for the average of the first six peaks detected for each channel.

For the conduction velocity (Fig. 3), the fact that the distance between successive electrodes as well as the activation times were known, allowed the wave velocity to be readily determined (i.e. velocity = distance/time). Velocity components in both the x- and y-directions were calculated using successive electrodes along the same row or column, respectively. Matlab was then used to draw a contour map relating the resultant wave velocity to its position, again for the average of the first six peaks detected.

For the velocity vector (Fig. 4), using the X and Y components of the conduction velocity algorithm above, we could directly calculate and plot the magnitude and direction of the resultant velocity, as shown in the figure.

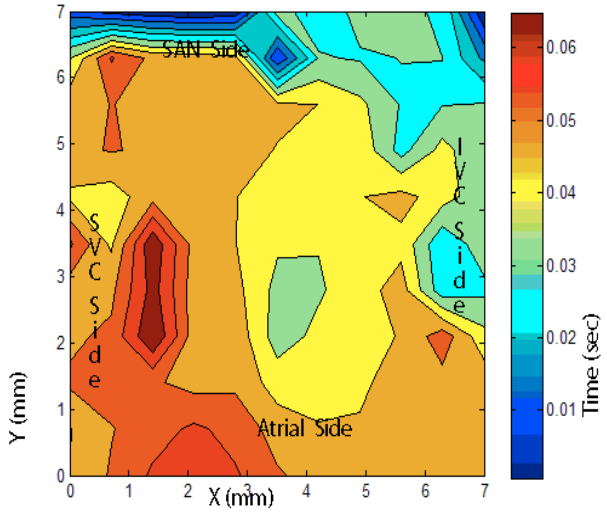

Fig. 2: SAN Activation Contour Map. The site of earliest activation is shown in the upper left hand corner. *SAN SIDE, ATRIAL SIDE, SVC SIDE and IVC SIDE: indicate sections of the tissue sample which are closest to the type of tissue identified*

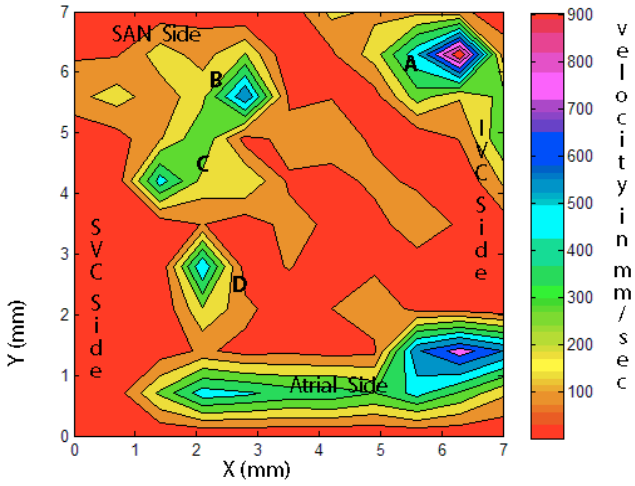

Fig. 3: SAN Conduction Velocity Map. For all abbreviations, refer to Fig. 2

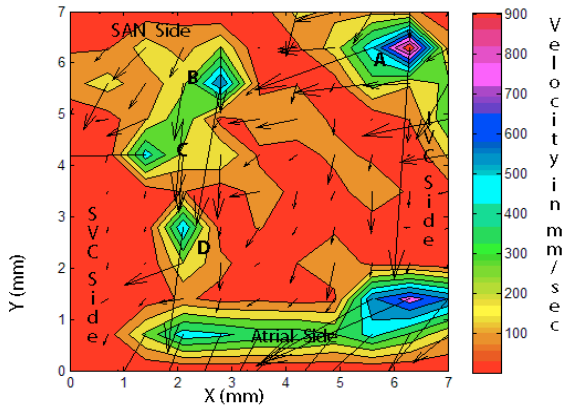

Fig. 4: SAN Velocity Vector Map. For all abbreviations, refer to Fig. 2.

III. Results

A. *Activation and Conduction Velocity Maps:*

The activation contour map (Fig. 2) revealed the relatively slow emergence of the extracellular AP from the site of pacemaker initiation, henceforth referred to as the SAN centre. The average AP velocity near the centre of the SAN was around 20-50 mm/s (Fig. 3). As the AP travelled towards the periphery of the SAN on the superior vena cava (SVC) side, there were pockets of tissue where the AP accelerated to about 200-500 mm/s (regions B, C & D in Fig. 3). The AP velocity appeared to stabilise at around 400-500 mm/s as it approached the periphery of the SAN. On the inferior vena cava (IVC) side, there were areas of high conductivity (region A, Fig. 3), with velocities as high as 700-800 mm/s. Conduction velocity tended to be slower and more steady on the IVC side than on the SVC side. The finding clearly shows scattered regions of high conductivity assisting the activation wavefront as it travels from the SAN centre to its periphery, especially on the SVC side.

The velocity vector map (Fig. 4) shows a tendency for the activation to propagate towards the SAN periphery, with increasing rates in some regions, such as A, B, C, D (Fig. 4), with a preferred path mostly via the SVC side.

B. *Extracellular SAN Waveforms:*

Another finding observed was the co-existence of different extracellular waveform shapes within the tissue [4]. Joyner *et* al [5] noted that the presence of electrical coupling between cells in the SAN and atrium creates 'transitional' action potential shapes near the border zone between the distinct SAN and atrial regions. This may indicate that between the SAN and its periphery, there are specific regions of myocytes where AP conduction is improved (refer to Fig. 3). Fig. 5 depicts the types of AP wave shapes, as determined from their extracellular monophasic potentials, and their locations within the electrode array. Extracellular waveform types, which may be an indication of the underlying AP waveshape, were categorised into four main types: a fully positive waveform (indicated by the red regions in Fig. 5), half-positive, half-negative waveform (indicated by the blue regions in Fig. 5), mostly negative waveform (indicated by the green regions in Fig. 5) and mostly positive waveform (indicated by the orange regions in Fig. 5). Electrode numbers and their respective locations in the array are also shown. Fig. 6 illustrates typical examples of the above extracellular waveform categories detected in the experiment. It was also observed that extracellular wavefronts tended to change shape slowly as they entered regions with different wavefront characteristics.

The AP wave appeared to begin from the centre of the SAN by having half positive and half negative form (Fig. 6A). It then intersperses with atrial-like cells which are positive (Fig. 6B). Near the SAN periphery, the wavefront encounters cells of different types where the waveforms are either mostly negative (Fig. 6C) or mostly positive (Fig. 6D). These 'transitional' myocytes may help to accelerate the AP as it travels from the SAN centre to the periphery (compare Fig. 5 with the velocity map of Fig. 3). Correlation algorithms were used in Matlab to find the locations of extracellular waveforms of similar shape.

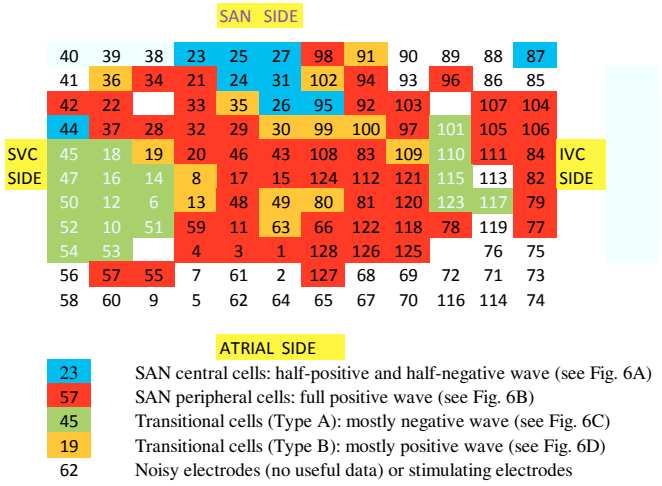

Fig.5: Extracellular wave types in the electrode matrix

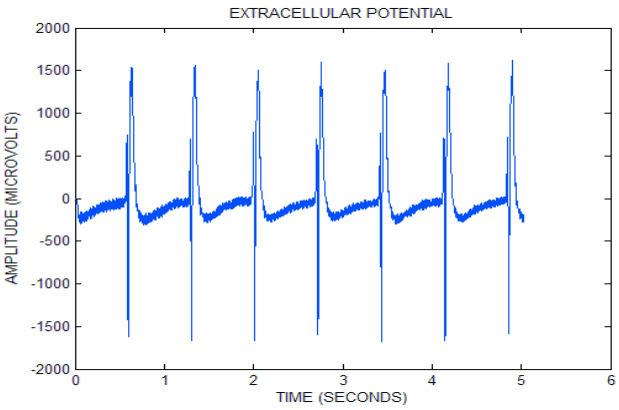

Fig. 6A: SAN central-type extracellular waveforms

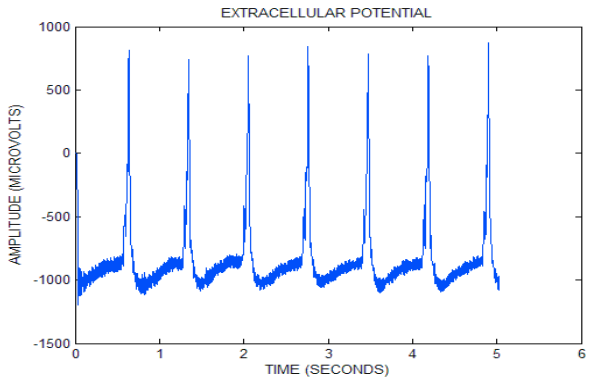

Fig. 6B: SAN peripheral-type extracellular waveforms

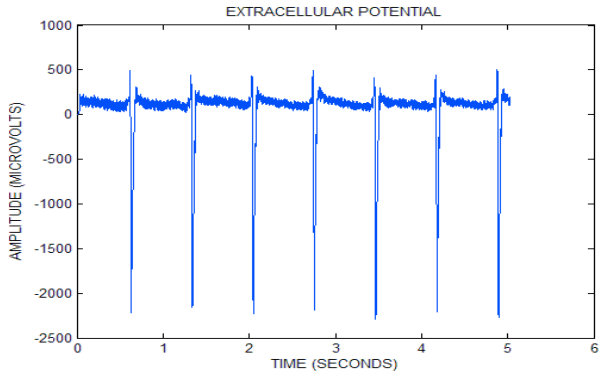

Fig. 6C: Transitional (Type A) extracellular waveforms

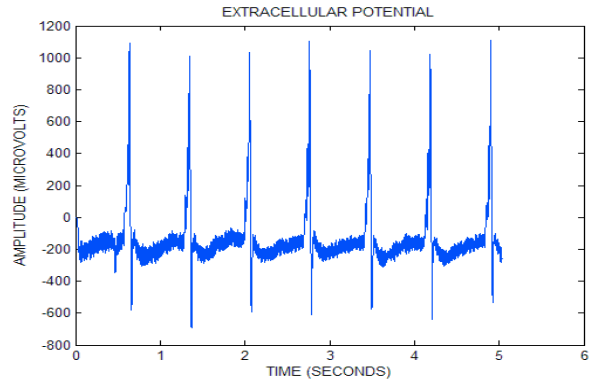

Fig. 6D: Transitional (Type B) extracellular waveforms

IV. DISCUSSIONS

The findings of this study support those of Sano and Yamagishi [6] indicating that APs emanating from the SAN are initially slow (around 20-50 mm/sec). As the activation wavefront travels towards the SAN periphery, it encounters tissue of varying conductivity, speeding up propagation to around 200-500 mm/s. In approaching the SAN periphery, the conduction velocity stabilises to around 400-500 mm/sec. The above study [6] also indicated that the preferred conduction path of activation was via the SVC, more so than via the IVC, a finding that has been confirmed by this study.

One possible explanation of the above findings is the fact that the size of the SAN is much smaller than the surrounding atrium. In order for the SAN to drive the atrium, it needs to have high impedance, demonstrated by an initial low conduction velocity (i.e. low conductivity), hence acting as a region of high impedance. The heterogeneous type of tissue between the SAN and its periphery enhances, to a certain extent, the conduction of the activation wavefront and facilitates the electrical interface between the SAN tissue, which offers high resistance to the propagation of APs, and its surroundings in the right atrium, which have much higher electrical conductivity. The findings may give credence to the *mosaic model* of myocyte configuration between the SAN and the atrium.

V. CONCLUSIONS AND FUTURE WORK

The experiments carried out in this study affirmed preliminary modelling and experimental results obtained earlier in regards to conduction velocity of SAN activation and the preferred activation paths within the SAN. From the above results, parameters, such as conductivity, could be deduced and used in future modelling studies.

An enhancement to the present system would be to use a 256-channel electrode array system to examine even a larger tissue sample of the SAN and its periphery. A further trial would be to conduct experiments in which both extracellular as well as intracellular SAN action potentials could be recorded. Intracellular potentials could be measured using optical dyes [7]. This will produce desirable parameters, such as intra and extracellular tissue conductivities, for a bidomain model implementation of the SAN.

REFERENCES

[1] S. Cloherty, S. Dokos and N. Lovell, *Qualitative Support for the Gradient Model of Cardiac Pacemaker Heterogeneity*, Proceedings of the 2005 IEEE, EMBC 27th Annual Conference, Shanghai, China, Sep. 1-4, 2005.

[2] H. Zhang, A.V. Holden and M.R. Boyett, *Gradient Model Versus Mosaic Model of the Sino-atrial Node*, J. of the American Heart Assoc., 2001, 103: 584-588.

[3] R.C. Barr and M.S. Spach, *Sampling Rates Required for Digital Reading of Intracellular and Extracellular Cardiac Potentials*, J. of the American Heart Assoc., 1977, 55: 40-48.

[4] M. Cramer, M. Siegal, T.J. Bigger, Jr., and B.F. Hoffman, *Characteristics of Extracellular Potentials Recorded from the Sinoatrial Pacemaker of the Rabbit*, J. of the American Heart Assoc., 1977, 41: 292-300.

[5] R. Joyner and F. Van Capelle, *Propagation through Electrically-Coupled Cells. How a Small SA Node Drives a Large Atrium*, J. of Biophysical Society, Volume 50, Dec 1986, 1157-1164.

[6] T. Sano and S. Yamagishi, *Spread of Excitation from the Sinus Node,* J. of the American Heart Assoc., 1965, 16: 423-430.

[7] G. Salama and B. Choi, *Images of Action Potential Propagation in Heart*, Physiology, 2000, 15: 33-41.